

Reassessment of $\text{TiN(s)} = \underline{\text{Ti}} + \underline{\text{N}}$ Equilibration in Liquid Iron

Jung-Mock JANG,¹⁾ Seok-Hyo SEO,¹⁾ Joon-Suk HAN,¹⁾ Dong-Sik KIM,¹⁾ Youn-Bae KANG²⁾ and Jong-Jin PAK^{1)*}

1) Department of Materials Engineering, Hanyang University, ERICA, Ansan, 426-791 Korea.

2) Graduate Institute of Ferrous Technology, Pohang University of Science and Technology (POSTECH), Pohang, 790-784 Korea.

(Received on May 18, 2015; accepted on August 3, 2015)

Thermodynamics of nitrogen solubility and TiN formation in liquid Fe–Ti alloys was reassessed over the temperature range from 1 823 to 1 973 K by combining new experimental data for the Ti–N–TiN relations in liquid iron at 1 823–1 873 K together with the authors' previous data. Using the Wagner's Interaction Parameter Formalism(WIPF), the first-order interaction parameters of e_{N}^{Ti} , e_{Ti}^{N} and $e_{\text{Ti}}^{\text{Ti}}$, and the equilibrium constant for the TiN formation reaction in liquid iron, $\log K_{\text{TiN}}$ were newly determined. The interaction parameters showed no temperature dependence in this temperature range. The calculated solubility product of titanium and nitrogen for TiN formation in liquid iron was in excellent agreement with the available experimental results measured at various temperatures.

KEY WORDS: titanium; nitrogen; TiN; interaction parameter.

1. Introduction

Titanium is often added in liquid steel during secondary refining process for various steel products to improve mechanical properties and corrosion resistance.^{1,2)} On the other hand, an excessive formation of TiN inclusions in liquid steel can cause a nozzle clogging problem during continuous casting and various defects in final products.³⁾ In particular, the deleterious effect of 6 μm TiN inclusion on the fatigue life of steel is equivalent to the harm of a 25 μm oxide inclusion.⁴⁾

In order to control TiN inclusion formation based on the supersaturation of [Ti] and [N] in liquid steel during cooling and casting processes, it is essential to have accurate information on thermodynamics of titanium, nitrogen and TiN formation in liquid iron over a wide range of melt temperature. In spite of such importance, there are still some uncertainties in the literature values including the recommended values of the Japan Society for the Promotion of Science (JSPS).⁵⁾ Furthermore, the recommended values of JSPS for the equilibrium constant, K_{TiN} for the formation of TiN and the interaction parameter values of e_{N}^{Ti} and e_{Ti}^{N} in liquid iron were taken from different sources^{6,7)} in which the data were determined by different experimental systems. This situation will cause significant errors in predicting the reaction equilibrium of TiN formation in Fe–Ti–N melt. In the authors' recent study,⁸⁾ the thermodynamics of Fe–Ti–N–TiN system was studied using the metal-gas and the metal-gas-nitride equilibration technique in the temperature range from 1 873 to 1 973 K, and an extensive discussion on the accuracy of those thermodynamic parameters has been carried out. Later the similar studies were carried out for Fe–Ti–Al–N, Fe–Ti–Cr–N, Fe–Ti–Mo–N and Fe–Ti–Nb–N

alloys at the same temperature range.^{9–11)} The accumulation of experimental data allowed us to obtain more reliable data on the thermodynamics of Fe–Ti–N–TiN system.

In the present study, the interaction parameters between titanium and nitrogen, and the equilibrium constant for the formation of TiN in liquid iron were reassessed over the temperature range from 1 823 to 1 973 K by combining new experimental data for the Ti–N–TiN relations in liquid iron at 1 823–1 873 K together with the authors' previous data.^{8–11)}

2. Experimental

The metal-gas and metal-nitride-gas equilibration experiments were carried out to determine the thermodynamics of titanium, nitrogen and TiN formation in Fe–Ti–N melts. Detailed descriptions of the experimental apparatus and procedure are available in the authors' recent studies.^{8–11)} Five hundred grams of high purity electrolytic iron (99.99 mass% purity, 60 mass ppm O, <5 mass ppm N, 18 mass ppm C, <5 mass ppm Si, <7 mass ppm Ni, 1 mass ppm Al) contained in an Al_2O_3 or MgO crucible was melted in the temperature range from 1 823 to 1 873 K by a high frequency induction furnace. Prior to the nitrogen solubility measurement, the iron melt was deoxidized by an Ar-10% H_2 gas blown onto the melt surface at a high flow rate of ~5 000 ml/min for 2 h. The oxygen content in the melt decreased to a value less than 20 mass ppm. The nitrogen partial pressure in the system was controlled by a mixture of Ar-10% H_2 and N_2 gases.

Strong agitation of the melt by an induction furnace resulted in a fast attainment of equilibrium nitrogen solubility in liquid iron under a nitrogen partial pressure within 1 h. This was confirmed by samplings and *in-situ* analysis for nitrogen content in the metal samples. Pellets of titanium (99.99 mass% purity) were added into liquid iron through an 18 mm ID quartz tube after confirming the equilibrium

* Corresponding author: E-mail: jjpak@hanyang.ac.kr

DOI: <http://dx.doi.org/10.2355/isijinternational.ISIJINT-2015-265>

nitrogen solubility in pure liquid iron under a nitrogen partial pressure. After each titanium addition, new nitrogen solubility equilibrium was attained within 1 h. Titanium addition and sampling were repeated until a stable TiN layer was formed on the surface of the iron melt. The formation of TiN in the iron melt could be also confirmed by a sharp decrease in nitrogen content checked by the analysis of metal samples during the experiment. In author's previous studies,⁸⁻¹¹⁾ the detailed procedure for chemical analysis is available.

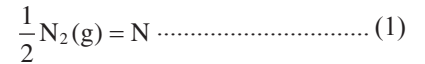
3. Results and Discussion

3.1. Effect of Titanium on Nitrogen Solubility in Liquid Iron

Table 1 summarizes the present experimental results of nitrogen solubility measurement with titanium additions in

liquid iron. **Figure 1** shows the variation of equilibrium nitrogen solubility in liquid iron with titanium additions under different nitrogen partial pressures at 1 823 and 1 873 K. The nitrogen solubility increases linearly as the titanium content increases in liquid iron when the melt is not saturated with TiN as shown as open symbols in the figure. When TiN is formed at higher Ti contents, the nitrogen solubility decreased significantly as shown as solid symbols in the figure. The Ti–N relation in liquid iron was not affected by the crucible material of Al₂O₃ or MgO.

The dissolution of nitrogen before the saturation of TiN in liquid iron can be written as



$$\Delta G_1^\circ = 3\,598 + 23.89T \text{ J/mol}^{12)}$$

Table 1. Experimental results of Ti and N Equilibration in liquid iron.

Temp (K)	P _{N₂} (atm)	Crucible	[% Ti]	[% N]	[% O]	[% Si]	[% Al]	[% Mg]	Saturation			
1 823	0.05	MgO	0	0.0100	0.0017	0.0049	–	0.0007				
			0.02	0.0100	0.0008	0.0042	–	0.0003				
			0.04	0.0102	0.0011	0.0038	–	0.0004				
			0.06	0.0103	0.0005	0.0045	–	0.0005				
			0.08	0.0103	0.0006	0.0048	–	0.0001				
			0.10	0.0104	0.0006	0.0036	–	0.0012				
			0.11	0.0105	0.0005	0.0012	–	0.0005				
			0.12	0.0104	0.0008	0.0036	–	0.0003	TiN			
			0.19	0.0068	0.0007	0.0047	–	0.0007	TiN			
	0.24	0.0053	0.0004	0.0021	–	0.0002	TiN					
	0.2	Al ₂ O ₃	0	0.0199	0.0007	0.0023	0.0008	–				
			0.02	0.0202	0.0013	0.0037	0.0001	–				
			0.05	0.0205	0.0010	0.0047	0.0011	–				
			0.06	0.0202	0.0007	0.0034	0.0007	–	TiN			
			0.13	0.0097	0.0005	0.0014	0.0003	–	TiN			
			0.18	0.0068	0.0008	0.0031	0.0003	–	TiN			
			1873	0.3	MgO	0	0.0242	0.0018	0.0042	–	0.0005	
						0.022	0.0243	0.0016	0.0021	–	0.0005	
0.045						0.0250	0.0014	0.0027	–	0.0007		
0.066	0.0257	0.0014				0.0032	–	0.0008				
0.075	0.0260	0.0018				0.0014	–	0.0013	TiN			
Al ₂ O ₃	0.077	0.0259			0.0011	0.0015	–	0.0005	TiN			
	0.091	0.0201			0.0009	0.0008	–	0.0009	TiN			
	0.094	0.0192			0.0009	0.0021	–	0.0009	TiN			
	0.109	0.0179			0.0007	0.0015	–	0.0005	TiN			
	0	0.0246			0.0018	0.0032	0.0002	–				
0.03	0.0247	0.0018	0.0044	0.0007	–							
0.05	0.0255	0.0016	0.0038	0.0015	–							
0.07	0.0258	0.0018	0.0045	0.0002	–							
0.08	0.0250	0.0020	0.0048	0.0009	–	TiN						
0.09	0.0208	0.0016	0.0036	0.0002	–	TiN						
0.11	0.0166	0.0019	0.0036	0.0007	–	TiN						
0.14	0.0139	0.0007	0.0047	0.0018	–	TiN						

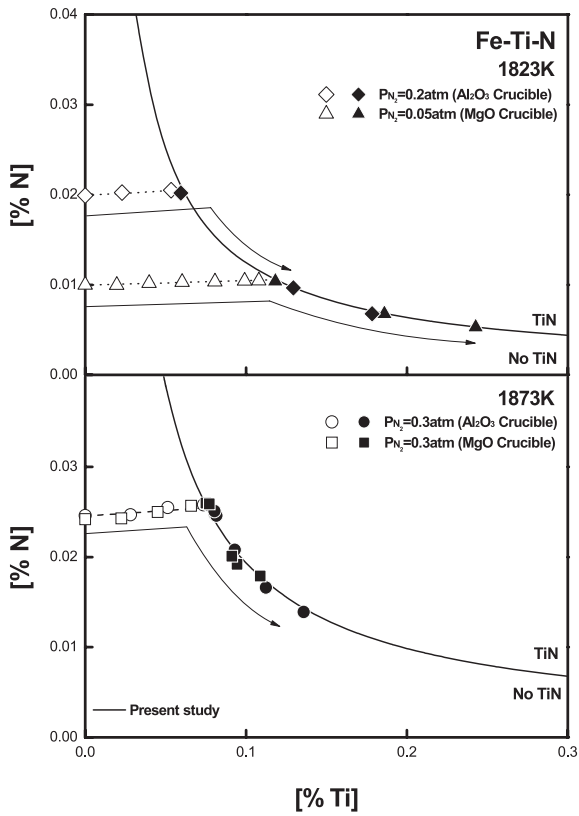


Fig. 1. Equilibrium [%Ti]-[%N] relation in Fe-Ti-N melts at 1823–1873 K.

$$K_N = \frac{f_N [\%N]}{P_{N_2}^{1/2}} \dots\dots\dots (2)$$

where K_N is the equilibrium constant for Reaction (1), [%N] is the equilibrium nitrogen content in mass% and, f_N is the activity coefficient of nitrogen in the 1 mass% standard state in liquid iron. P_{N_2} is the nitrogen partial pressure in atm over the melt surface.

In Fe-Ti-N alloy melts, the Wagner's Interaction Parameter Formalism (WIPF) can be used to estimate the f_N in Eq. (2) along with first-order interaction parameters as:

$$\log f_N = e_N^{Ti} [\%Ti] + e_N^N [\%N] = \log K_1 - \log [\%N] + \frac{1}{2} \log P_{N_2} \dots (3)$$

where the value of e_N^N is known to be 0 in the present experimental temperature range.¹³⁾ As mentioned earlier, the oxygen content in the melt was very low, and the effect of oxygen on nitrogen was assumed to be negligible. Silicon, aluminum and magnesium contents in the melt were less than 50, 18 and 13 mass ppm, respectively, and the effects of those elements can be also neglected.

Figure 2 shows the relation of $\log f_N$ vs titanium content in mass% in liquid iron using the relation expressed by Eq. (3) from the nitrogen solubility data determined in the present study at 1823–1873 K together with the data determined in the authors' recent studies at 1873–1973 K.^{8,9)} The results determined at various temperatures and nitrogen partial pressures show excellent linear relationships up to 0.19 mass% Ti and the e_N^{Ti} value determined by the linear regression analysis of the data is -0.21 at all temperatures as shown in the figure. Discrepancy of experimental data obtained at low temperatures was less than those obtained at

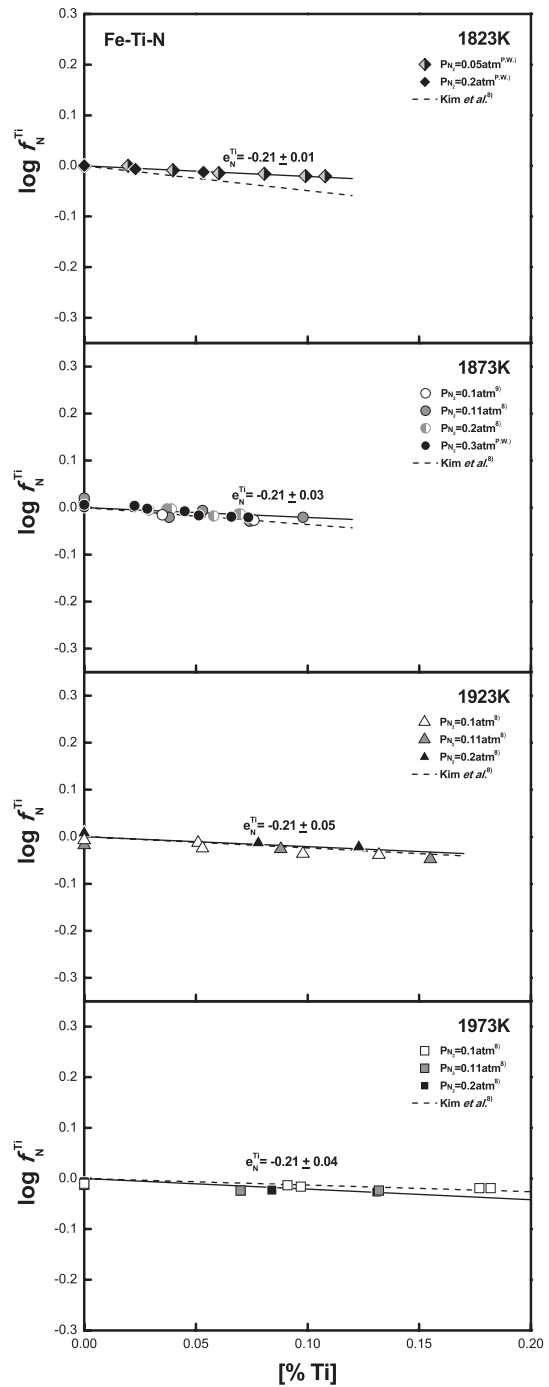


Fig. 2. Relation of $\log f_N^{Ti}$ vs. [%Ti] in Fe-Ti-N melts at 1823–1973 K.

high temperatures. The standard deviations for the interaction parameter determined at each temperature are shown in Fig. 2. Temperature dependence was not evaluated for this parameter because it was found to be within experimental uncertainties. The dotted lines in Fig. 2 show the calculated relations using the e_N^{Ti} values ($= -8507/T + 4.18$) determined in the temperature range of 1873–1973 K by Kim *et al.*⁸⁾ The discrepancy of e_N^{Ti} value is significant at a 1823 K.

Figure 3 shows the same relation for the data determined at all temperatures. The e_N^{Ti} value of -0.21 ± 0.016 can be determined by the linear regression analysis and it gives an excellent correlation of data for all temperatures. Using the WIPF's reciprocal relationship,¹⁴⁾ the value of e_N^N can be evaluated as -0.728 ± 0.044 . Figure 3 also compares the

relations determined by previous workers at 1 873 K, and there is huge scatter among their e_N^{Ti} values from -0.36 to -0.87 .^{6,8,15,17} They all reported temperature dependence of the e_N^{Ti} values as shown in **Table 2**.

In the present study, a constant e_N^{Ti} value of -0.21 was obtained in the temperature range of 1 823–1 973 K without noticeable temperature dependence. The accuracy of the e_N^{Ti} value is important in studying thermodynamics of $TiN(s) = \underline{Ti} + \underline{N}$ equilibrium in liquid iron. The validity of e_N^{Ti} values determined in the present study will be discussed more in detail in the next section.

3.2. TiN Formation in Liquid Iron

The solubility product of titanium and nitrogen in liquid iron for TiN saturation can be determined as shown as solid

symbols in Fig. 1. The reaction equilibrium for the formation of pure solid TiN in liquid iron is



$$K_{TiN} = \frac{h_{Ti}h_N}{a_{TiN}} = f_{Ti}f_N[\%Ti][\%N] \dots\dots\dots (5)$$

The equilibrium constant of the reaction (4) can be expressed as

$$\begin{aligned} \log K_{TiN} &= -\frac{\Delta G^\circ}{2.303RT} = \log h_{Ti} \cdot h_N \\ &= \log f_{Ti} + \log f_N + \log [\%Ti][\%N] \\ &= e_{Ti}^{Ti}[\%Ti] + e_N^{Ti}[\%N] + e_N^{Ti}[\%Ti] + \log [\%Ti][\%N] \end{aligned} \dots\dots\dots (6)$$

where h_i and f_i are the activity and activity coefficient of i in liquid iron with respect to 1 mass% standard state, respectively. e_{Ti}^{Ti} is the first-order self-interaction parameter of titanium in liquid iron and, the values of e_N^{Ti} and e_{Ti}^{Ti} were determined in the preceding section. The TiN formed in the melt was identified as a pure solid stoichiometric TiN by the XRD analysis.^{8–11} Therefore, the activity of TiN is unity under the present experimental condition.

Then, Eq. (6) can be rearranged as

$$-e_N^{Ti}[\%N] - e_{Ti}^{Ti}[\%Ti] - \log [\%Ti][\%N] = e_{Ti}^{Ti}[\%Ti] - \log K_{TiN} \dots\dots\dots (7)$$

The left hand side of Eq. (7) can be plotted *versus* [%Ti], and the e_{Ti}^{Ti} and the $\log K_{TiN}$ values are simultaneously obtained by taking the slope and the intercept at y-axis of

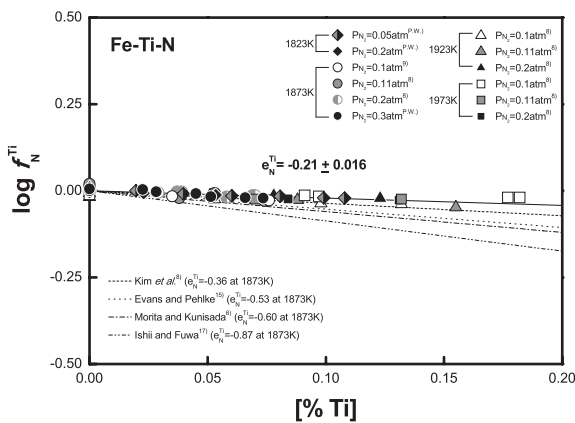


Fig. 3. Relation of $\log f_N^{Ti}$ vs. [%Ti] in Fe–Ti–N melts together with previous results.

Table 2. Thermodynamic parameters of Ti and N in liquid iron at 1 873 K.

e_N^{Ti} (Temp. Dependency)	e_{Ti}^{Ti} (Temp. Dependency)	$\log K_{TiN}$ (Temp. Dependency)	Temp. (K)	[% Ti] range	Method	Ref.
-0.21	0.048	-2.742 (-12 740/T+4.06)	1 823–1 973	<0.52	Sampling (Fe–Ti–N)	Present study
-0.36 (-8 507/T+4.18)	0.048	-2.792 (-15 780/T+5.63)	1 873–1 973	<0.52	Sampling (Fe–Ti–N)	8
*-0.60 (-5 700/T+2.45)	0.53 (1 873 K) 0.29 (1 923 K) 0.26 (1 973 K)	*-2.760 (-19 800/T+7.78)	1 873–1 973	<0.5	Sampling (Fe–Ti–N)	6
-0.53 (-6 200/T+2.7)		-2.584 (-16 433/T+6.19)	1 873–2 023	<0.32	Sieverts (Fe–Ti–N)	15
-0.63			1 973	<0.3	Sampling (Fe–Ti–N)	16
-0.87 (-7 240/T+3.0)			1 853–1 953	<0.25	Sampling (Fe–Ti–N)	17
	*0.048		1 873	<8.8	EMF (Fe–Ti–O)	7
	0.048		1 900	<1	Estimation from the data of Hadley <i>et al.</i> ²¹ and Kelly <i>et al.</i> ²² (Fe–Ti–O)	18
	0.042		1 873	<12	EMF (Fe–Ti–O)	19
	0.023		1 873	<2.1	Ag bath Iso-activity	20

(*: Recommended values of JSPS)

the plot, provided that the experimental data could be well represented by Eq. (7). One such plot is shown in Fig. 4 using the present experimental data for the TiN solubility product in liquid iron at 1 823 and 1 873 K together with the previous data determined in the authors' recent studies.^{8–11} As can be seen, the data points determined at different nitrogen partial pressures and temperatures show excellent linear relationships.

The $e_{\text{Ti}}^{\text{Ti}}$ value can be obtained as 0.048 ± 0.0024 from the slope of the lines in the temperature range from 1 823 to 1 973 K. Temperature dependence was not evaluated for this parameter within experimental uncertainties. The values of $\log K_{\text{TiN}}$ are obtained as -2.935 , -2.742 , -2.570 and -2.402 at 1 823, 1 873, 1 923 and 1 973 K, respectively. The temperature dependence of $\log K_{\text{TiN}}$ is shown in Fig. 5, and it can be expressed as $-12\,740/T + 4.06$. The standard Gibbs free energy change of Reaction (4) is then obtained as

$$\Delta G_{\text{TiN}}^{\circ} = 244\,000 - 77.7T \text{ J/mol} \dots\dots\dots (8)$$

In the present study, three important thermodynamic variables of e_{N}^{Ti} , $e_{\text{Ti}}^{\text{Ti}}$ and $\log K_{\text{TiN}}$ were determined simultaneously in one consistent experimental method over the temperature range from 1 823 to 1 973 K by combining new experimental data for the Ti–N–TiN relations in liquid iron at 1 823–1 873 K together with the authors' previous data at 1 873–1 973 K.^{8–11} The first-order interaction parameters apparently showed no temperature dependence in this

temperature range, and the $\log K_{\text{TiN}}$ values showed a less temperature dependence compared to the previous results as shown in Fig. 4.

An extensive discussion on those thermodynamic parameters has been carried out in the authors' previous study.⁸ Morita and Kunisada⁶ reported their own combination of $e_{\text{Ti}}^{\text{Ti}}$ and $\log K_{\text{TiN}}$ values in order to best represent their experimental data measured by the similar method using an induction furnace as the present study. They reported the $e_{\text{Ti}}^{\text{Ti}}$ values in liquid iron as 0.53, 0.29 and 0.26 at 1 873, 1 923 and 1 973 K, respectively, along with the $e_{\text{N}}^{\text{Ti}} = -5\,700/T + 2.45$ as shown in Table 2. The $e_{\text{Ti}}^{\text{Ti}}$ values in liquid iron determined by various authors are compared in Table 2.^{6–8,18–20} In spite of different experimental techniques, the values of $e_{\text{Ti}}^{\text{Ti}}$ are quite well agreed in the range of 0.042–0.048 at 1 873 K except for the values obtained by Morita and Kunisada⁶ and Yuanchang *et al.*²⁰ The recommended value for $e_{\text{Ti}}^{\text{Ti}}$ in JSPS (= 0.048 at 1 873 K) was taken from the data of Janke and Fischer⁷ who studied the titanium deoxidation equilibrium in liquid iron by the EMF method. The $e_{\text{Ti}}^{\text{Ti}}$ value of 0.048 at 1 823–1 973 K determined in Fe–Ti–N system in the present study is well agreed with the values determined in Fe–Ti–O system.^{7,18,19}

Figure 6 compares the available experimental results^{6,8–11,15,17} and the predictions of equilibrium solubility product of titanium and nitrogen for TiN formation in liquid iron in the temperature range of 1 823–1 973 K. The lines were calculated using Eq. (7) from $\log K_{\text{TiN}}$ and interaction parameters determined by the present study and other workers^{6,8,15} including the recommended values of JSPS⁵ as shown in Table 2.

The experimental data for TiN solubility product in liquid iron measured at 1 823 K are in excellent agreement with the solid line calculated in the present study. The dotted line calculated at the same temperature using the parameters determined by the author's previous study⁸ is lower than the experimental data at Ti content less than 0.3 mass%. At 1 873 K, the experimental data and the calculated lines are well agreed among various researchers^{5,6,8} except Evans and Pehlke's data.¹⁵ Evans and Pehlke¹⁵ measured the solubility product of titanium and nitrogen for TiN formation in liquid Fe–Ti alloys by the Sieverts' method in the temperature range of 1 873–2 023 K, by determining the break points in the Sieverts' law lines of nitrogen solubility for the precipitation of TiN with increasing nitrogen partial pressure. As shown in the figure, the solubility product data measured by the Sieverts' method shows significantly higher values than the data measured by the sampling method. As pointed out by Pehlke and Elliott in their earlier work with Fe–Ti melts,¹² the formation of a stable nitride in the sieverts chamber would increase the apparent absorption of nitrogen.

The calculated lines at 1 823–1 973 K using the recommended values in JSPS are not in agreement with any of those experimental data.^{6,8–11,17} As mentioned earlier, the recommended values of e_{N}^{Ti} , $e_{\text{Ti}}^{\text{Ti}}$ and $\log K_{\text{TiN}}$ in JSPS were taken from the different sources^{6,7} where those data were determined by completely different experimental techniques. This may cause errors in predicting the reaction equilibrium in Fe–Ti–N melts.

At 1 873 K, the solubility product data measured by Morita and Kunisada⁶ are in excellent agreement with the

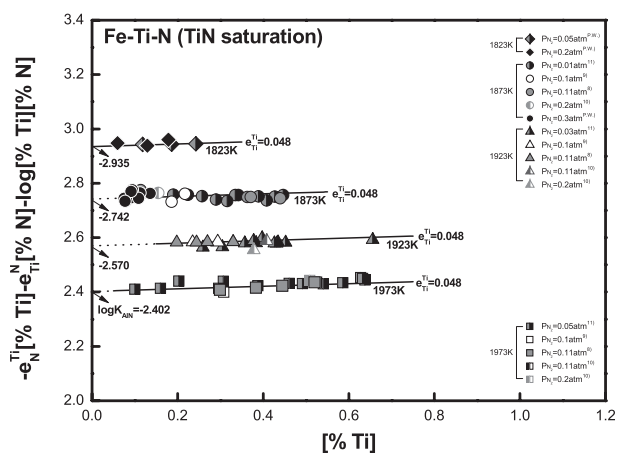


Fig. 4. Relation of Eq. (7) to determine $e_{\text{Ti}}^{\text{Ti}}$ and $\log K_{\text{TiN}}$ values.

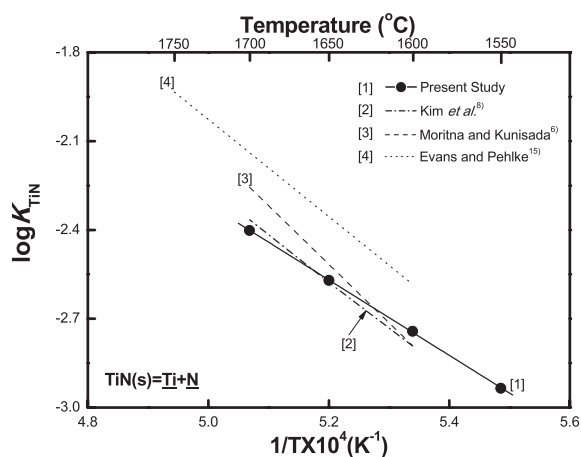


Fig. 5. Temperature dependence of $\log K_{\text{TiN}}$ values.

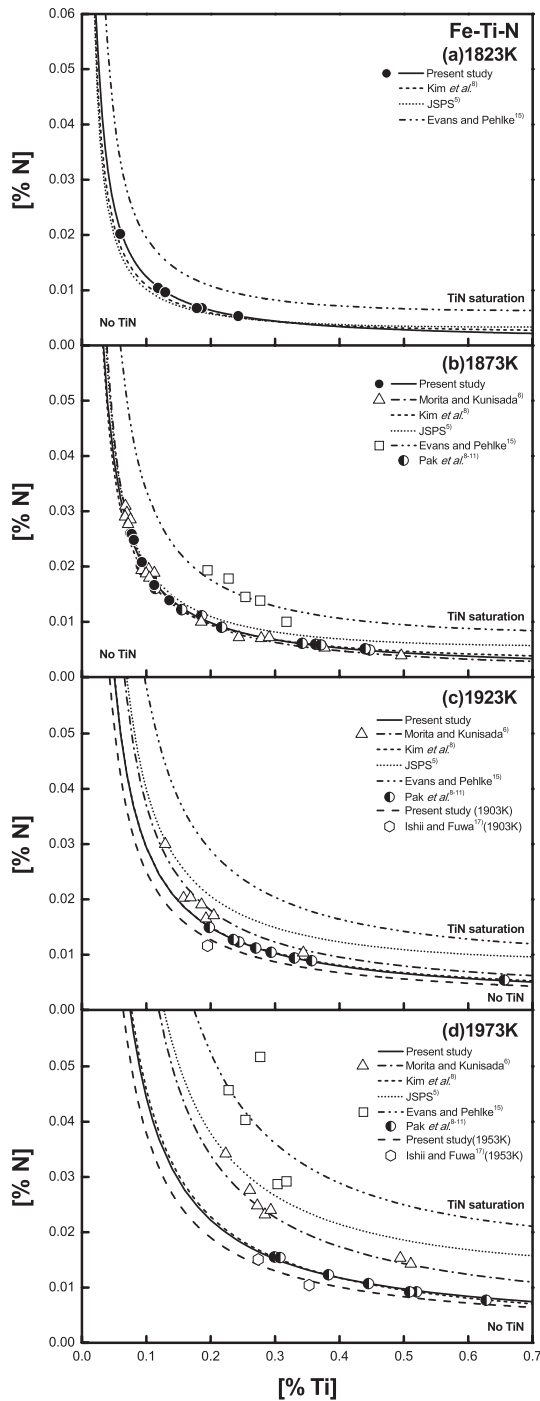


Fig. 6. Equilibrium [%Ti]-[%N] relations in Fe-Ti-N melts saturated with TiN at (a) 1 823, (b) 1 873, (c) 1 923 and (d) 1 973 K.

present author’s results.^{8–11)} However, at 1 923 and 1 973 K, the solubility product data and predicted lines of Morita and Kunisada⁶⁾ are higher than those determined in the present study although the experimental methods are very similar. In the Morita and Kunisada’s study, they measured the melt temperature indirectly by a thermocouple located at the bottom of crucible. In the present author’s study, the melt temperature was directly monitored by the immersion of an alumina sheathed thermocouple, and it was controlled within 2 K during experiment by the PID controller of the induction furnace. Figure 6 also shows the solubility product data measured by Ishii and Fuwa¹⁷⁾ at 1 903 and 1 953 K. They are in excellent agreement with the solubility product

lines at the same temperatures calculated using the thermodynamic data determined in the present study.

3.3. Temperature Dependence of Interaction Parameters

In the preceding sections, important thermodynamic interaction parameters of e_N^{Ti} and e_{Ti}^{Ti} were determined in the temperature range from 1 823–1 973 K. They apparently showed no temperature dependence in this temperature range. However, one may expect that any thermodynamic variables have temperature dependence by their inherent nature. In this section, the temperature dependence of interaction parameters is briefly discussed.

According to Darken’s quadratic formalism,^{21,22)} in a binary system 1-2 where “1” is the solvent, Gibbs energy of the binary solution in a dilute region for the solute “2” can be expressed by the following equation.

$$g = X_1 g_1^\circ + X_2 (g_2^\circ + C_2) + RT(X_1 \ln X_1 + X_2 \ln X_2) + \alpha_{12} X_1 X_2 \dots \dots \dots (9)$$

where C_2 is introduced to change the standard state of 2 from Raoultian to Henrian, and α_{12} is an interaction energy between 1 and 2, and can be represented by:

$$\alpha_{12} = h_{12} - T s_{12} \dots \dots \dots (10)$$

where h_{12} and s_{12} are related to the excess enthalpy and the excess entropy, respectively.

The excess Gibbs energy is therefore:

$$g^{ex} = \alpha_{12} X_1 X_2 + C_2 X_2 \dots \dots \dots (11)$$

From the definition of the excess Gibbs energy in the binary 1–2 system

$$g^{ex} = RT(X_1 \ln \gamma_1 + X_2 \ln \gamma_2) \dots \dots \dots (12)$$

By differentiation of the Eq. (11) assuming h_{12} and s_{12} are constants, and by comparison with the Eq. (12), one obtains:

$$RT \ln \gamma_1 = \alpha_{12} X_2^2 \dots \dots \dots (13)$$

$$RT \ln \gamma_2 = C_2 + \alpha_{12} (1 - 2X_2 + X_2^2) \dots \dots \dots (14)$$

As $\ln \gamma_2 = \ln \gamma_2^\circ + \varepsilon_2^2 X_2 + \rho_2^2 X_2^2$, and neglecting the second order term,

$$\varepsilon_2^2 = -\frac{2\alpha_{12}}{RT} = -\frac{2(h_{12} - T s_{12})}{RT} \dots \dots \dots (15)$$

The ε_2^2 is converted by utilizing the following relations derived Lupis,²³⁾ where “1” denotes the solvent.

$$e_2^2 = \frac{1}{230} \left(\frac{M_1}{M_2} \varepsilon_2^2 - \frac{M_1 - M_2}{M_2} \right) \dots \dots \dots (16)$$

$$= -\frac{2}{230} \left(\frac{M_1}{M_2} \cdot \frac{h_{12}}{R} \right) \frac{1}{T} + \frac{2}{230} \left(\frac{M_1}{M_2} \cdot \frac{s_{12}}{R} \right) - \frac{M_1 - M_2}{230 M_2} \dots (17)$$

The temperature dependence of the e_2^2 is

$$\frac{de_2^2}{d(1/T)} = -\frac{2}{230} \left(\frac{M_1}{M_2} \right) \left(\frac{h_{12}}{R} \right) \dots \dots \dots (18)$$

Similarly, in a 1–2–3 ternary solution, the excess Gibbs energy can be expressed by the following equation.^{21,22)}

$$g^{ex} = C_2 X_2 + C_3 X_3 + \alpha_{12} X_1 X_2 + \alpha_{23} X_2 X_3 + \alpha_{31} X_3 X_1 \dots (19)$$

and by following similar steps shown for the binary solution,

$$RT\ln\gamma_1 = \alpha_{12}X_2^2 + \alpha_{31}X_3^2 + (\alpha_{12} + \alpha_{31} - \alpha_{23})X_2X_3 \dots\dots\dots (20)$$

$$RT\ln\gamma_2 = (\alpha_{12} + C_2) - 2\alpha_{12}X_2 - (\alpha_{12} + \alpha_{31} - \alpha_{23})X_3 + [\alpha_{12}X_2^2 + \alpha_{31}X_3^2 + (\alpha_{12} + \alpha_{31} - \alpha_{23})X_2X_3] \dots\dots (21)$$

$$RT\ln\gamma_3 = (\alpha_{31} + C_3) - 2\alpha_{31}X_3 - (\alpha_{12} + \alpha_{31} - \alpha_{23})X_2 + [\alpha_{12}X_2^2 + \alpha_{31}X_3^2 + (\alpha_{12} + \alpha_{31} - \alpha_{23})X_2X_3] \dots\dots (22)$$

where $-\frac{(\alpha_{12} + \alpha_{31} - \alpha_{23})}{RT}$ corresponds to ε_2^3 which can be expressed by the following equation:

$$\varepsilon_2^3 = -\frac{(\alpha_{12} + \alpha_{31} - \alpha_{23})}{RT} \dots\dots\dots (23)$$

$$= -\frac{(h_{12} - T\delta_{12}) + (h_{31} - T\delta_{31}) - (h_{23} - T\delta_{23})}{RT} \dots\dots\dots (24)$$

$$= -\frac{h_{12} + h_{31} - h_{23}}{R} \frac{1}{T} + \frac{s_{12} + s_{31} - s_{23}}{R} \dots\dots\dots (25)$$

When, Fe, Ti and N are substituted into 1, 2 and 3, respectively, ε_{Ti}^N becomes:

$$\varepsilon_{Ti}^N = -\frac{h_{FeTi} + h_{FeN} - h_{TiN}}{R} \frac{1}{T} + \frac{s_{FeTi} + s_{FeN} - s_{TiN}}{R} = \varepsilon_{Ti}^N \dots\dots (26)$$

The e_N^{Ti} is expressed as:

$$e_N^{Ti} = \frac{1}{230} \left(\frac{M_{Fe}}{M_{Ti}} \varepsilon_{Ti}^N - \frac{M_{Fe} - M_{Ti}}{M_{Ti}} \right) \dots\dots\dots (27)$$

$$= -\frac{1}{230} \left(\frac{M_{Fe}}{M_{Ti}} \right) \left(\frac{h_{FeTi} + h_{FeN} - h_{TiN}}{R} \right) \frac{1}{T} + \frac{1}{230} \left(\frac{M_{Fe}}{M_{Ti}} \right) \left(\frac{s_{FeTi} + s_{FeN} - s_{TiN}}{R} \right) - \frac{M_{Fe} - M_{Ti}}{230M_{Ti}} \dots\dots (28)$$

Then, the temperature dependence of the e_N^{Ti} ($= A_{TiN}/T + B_{TiN}$) is

$$A_{TiN} = \frac{de_N^{Ti}}{d(1/T)} = -\frac{1}{230R} \left(\frac{M_{Fe}}{M_{Ti}} \right) (h_{FeTi} + h_{FeN} - h_{TiN}) \dots\dots (29)$$

Therefore, if $h_{FeTi} + h_{FeN} - h_{TiN} \approx 0$, then the temperature dependence of e_N^{Ti} becomes almost zero.

The values of h_{FeTi} , h_{FeN} and h_{TiN} have been reported in literature, but those are not just constant, but were expressed as functions on compositions.²⁴⁻²⁶ By differentiating the Eq. (19) taking into account the composition dependence of h_{FeTi} , h_{FeN} and h_{TiN} , the values corresponding to the term in the last parenthesis in the Eq. (29) becomes 772 kJ/mol. Inserting these values into the Eq. (29) gives the $A_{TiN} \approx -471$ J/mol. This value is not zero, but is much smaller than the reported values ($-8\ 507$,⁸ $-5\ 700$,⁶ $-6\ 200$ ¹⁵) and $-7\ 240$ J/mol¹⁷) as shown in Table 2). The above estimation assumes no ternary interaction in the Fe-Ti-N system.

The value estimated in this section shows the validity of e_N^{Ti} and e_{Ti}^N values with negligible temperature dependence determined in the present study, compared to those reported in the literature.^{6,8,15,17}

4. Conclusions

The values of Wagner's interaction parameters of e_N^{Ti} , e_{Ti}^N and e_{Ti}^{Ti} and the equilibrium constant for the TiN formation reaction in liquid iron, $\log K_{TiN}$ were newly determined over the temperature range from 1 823 to 1 973 K as follows:

$$e_N^{Ti} = -0.21 \pm 0.016$$

$$e_{Ti}^N = -0.728 \pm 0.044$$

$$e_{Ti}^{Ti} = 0.048 \pm 0.0024$$

$$\log K_{TiN} = -\frac{12\ 740}{T} + 4.06$$

Acknowledgments

This work was supported by the research fund of Hanyang University (HY-2013-P).

REFERENCES

- 1) C. Wang, H. Gao, Y. Dai, J. Wang and B. Sun: *Met. Mater. Int.*, **18** (2012), 47.
- 2) J. M. Kim and H. W. Lee: *Korean J. Met. Mater.*, **51** (2013), 829.
- 3) P. rocabois, J. Lehmann, C. Gatellier and J. P. Teres: *Ironmaking Steelmaking*, **30** (2003), 95.
- 4) J. Fu, J. Zhu, L. Di, F. S. Tong, D. L. Liu and Y. L. Wang: *Acta Metall. Sin.*, **36** (2000), 801.
- 5) *Steelmaking Data Sourcebook*, The Japan Society for Promotion of Science, The 19th Committee in Steelmaking, Gordon and Breach Science Publishers, Amsterdam, (1988), 217.
- 6) Z. Morita and K. Kunisada: *Tetsu-to-Hagané*, **63** (1977), 1663.
- 7) D. Janke and W. A. Fischer: *Arch. Eisenhüttenwes.*, **47** (1976), 195.
- 8) W. Y. Kim, J. O. Jo, T. I. Chung, D. S. Kim and J. J. Pak: *ISIJ Int.*, **47** (2007), 1082.
- 9) T. I. Chung, J. B. Lee, J. G. Kang, J. O. Jo, B. H. Kim and J. J. Pak: *Mater. Trans.*, **49** (2008), 854.
- 10) W. Y. Kim, J. O. Jo, C. O. Lee, D. S. Kim and J. J. Pak: *ISIJ Int.*, **48** (2008), 17.
- 11) J. O. Jo, W. Y. Kim, C. O. Lee and J. J. Pak: *ISIJ Int.*, **50** (2010), 1373.
- 12) R. D. Pehlke and J. F. Elliott: *Trans. Met. Soc. AIME*, **218** (1960), 1088.
- 13) A. Sieverts and G. Zapf: *Z. Phys. Chem. A. AIME*, **172** (1935), 314.
- 14) C. Wagner: *Thermodynamics of Alloys*, Addison-Wesley Press, Cambridge, MA, (1952), 47, 51.
- 15) D. B. Evans and R. D. Pehlke: *Trans. Metall. Soc. AIME*, **233** (1965), 1620.
- 16) S. Maekawa and Y. Nakagawa: *Tetsu-to-Hagané*, **46** (1960), 1438.
- 17) F. Ishii and T. Fuwa: *Tetsu-to-Hagané*, **68** (1982), 1560.
- 18) J. Chipman: *Trans. TMS-AIME*, **218** (1960), 767.
- 19) K. Suzuki and K. Sanbongi: *Trans. Iron Steel Inst. Jpn.*, **15** (1975), 618.
- 20) G. Yuanchang, W. Changzhen and Y. Hualong: *Metall. Trans. B*, **21B** (1990), 537.
- 21) L. S. Darken: *Trans. Metall. Soc. AIME*, **239** (1967), 80.
- 22) L. S. Darken: *Trans. Metall. Soc. AIME*, **239** (1967), 90.
- 23) C. H. P. Lupis: *Chemical Thermodynamics of Materials*, Elsevier Science, New York, NY, (1983), 184.
- 24) L. F. S. Dumitrescu, M. Hillert and N. Saunders: *J. Phase Equilibria*, **19** (1998), 441.
- 25) K. Frisk: *Calphad*, **15** (1991), 79.
- 26) B. J. Lee: *Metall. Trans. A*, **32A** (2001), 2423.